

# Density of states governs light scattering in photonic crystals

P.D. García,<sup>1</sup> R. Sapienza,<sup>1</sup> Luis S. Froufe-Pérez,<sup>1</sup> and C. López<sup>1</sup>

<sup>1</sup>*Instituto de Ciencia de Materiales de Madrid (CSIC) and Unidad Asociada CSIC-UVigo, Cantoblanco 28049 Madrid España.*

(Dated: November 1, 2018)

We describe a smooth transition from (fully ordered) photonic crystal to (fully disordered) photonic glass that enables us to make an accurate measurement of the scattering mean free path in nanostructured media and, in turn, establishes the dominant role of the density of states. We have found one order of magnitude chromatic variation in the scattering mean free path in photonic crystals for just  $\sim 3\%$  shift around the band-gap ( $\sim 27$  nm in wavelength).

PACS numbers: 42.25.Dd, 42.25.Fx, 42.70.Qs, 46.65.+g

Contemporary photonic science is capable of addressing fundamental questions at the basis of light-matter interactions, of which the role of the photon density of states,  $\mathcal{D}(\omega)$ , in nanostructured media is one of the most intriguing.

Artificially engineered materials allow the control of light transport through interference in the internal nanostructure, rather than on the refraction in the body boundaries, engendering new materials properties. Photonic crystals, in which the dielectric constant is periodically modulated, manipulate electromagnetic states and the available phase space and control fundamental aspects of light-matter interaction like light emission [1] and light transport [2], much like semiconductors control electrons. Redistribution and inhibition of the emission from photonic crystals was proven [3], but unconventional light transport in partially-disordered photonic crystals has only been hinted at by pioneering experiments [4, 5]. Other topologies, like random media [6], correlated disordered [7] or fractal [8], employ the aperiodic subwavelength dielectric nanostructure to achieve similar light control for transport [9] and random lasing emission [10].

Light scattering by weak topological disorder in a photonic crystal and the interplay between order and disorder has yet to be fully understood and explored. As an important step, the relation between scattering extinction and  $\mathcal{D}(\omega)$  has just been theoretically derived [11]. As pointed out by John [2] a dramatic change in light diffusion can occur for frequencies in or around the band-gap and eventually Anderson localisation of light can be reached, the photonic conductor becoming an insulator [12]. In the quest for light localization, the first experiments focused on fully random media [13], only recently transverse localization has been reported in two-dimensional crystals with disorder [14].

Even far from the localization regime, the scattering properties of Bloch modes, the periodic electromagnetic modes of a photonic crystal, are expected to be profoundly different from the diffusive modes encountered in conventional random media. Pioneering experiments on coherent backscattering [15], and diffuse light transport

[16, 17] in photonic crystals searched for signatures of Bloch-mode mediated scattering but have merely shown standard light diffusion. Moreover, the experiments have been interpreted using a model that assumes no photonic modal dispersion but rather a modified reflectivity at the system boundaries [18].

In this letter we study the scattering mean free path,  $\ell_s$ , the fundamental building block for any wave transport model, for the special case of photonic crystals with a controlled amount of disorder. We report experimental evidence of strong chromatic dispersion of  $\ell_s$  from band-edge to band-gap, and values of up to  $\sim 100 - 500 \mu\text{m}$ , i.e.  $\sim 300$  times the lattice parameter ( $a$ ), an order of magnitude higher than previously reported [15, 16, 17].

Single scattering events in a system with modified light modes and density of states, as in a photonic crystal, are very different from those occurring in vacuum due to: a) an increase of light-matter interaction and thus of scattering by defects, when  $\mathcal{D}(\omega)$  is increased at the vicinity of band-edges and b) a suppression of the scattering channels, i.e. a increase of  $\ell_s$  in the band-gap, where  $\mathcal{D}(\omega)$  is strongly reduced.

The scattering strength can be studied via simultaneous reflection and transmission measurements, when absorption is negligible (the absorption length  $\ell_a \sim 10$  m [19]) and for energies below the onset of diffraction ( $a/\lambda \sim 1.12$  [20] where  $\lambda$  is the light wavelength). We assume that scattering losses follow Lambert-Beer's law, i.e. that after a thickness  $L$ , a ballistic beam attenuates as  $I(L) = I_0 \exp(-L/\ell_s)$ . The intensity balance can then be expressed as

$$T(L) + R(L) = \exp(-L/\ell_s), \quad (1)$$

where  $T(L)$  and  $R(L)$  are the ballistic transmission and reflection as a function of sample thickness in a given direction.

The samples are Polymethyl-metacrilate (PMMA, refractive index,  $n = 1.49$ ) self-assembled face centred cubic (fcc) photonic crystals [21] with controlled density of intentionally added vacancies [7] (from 0% to 40%) (see Fig. 1a and 1b). These vacancies are obtained upon removal of given fractions of constituting spheres from

random lattice positions.

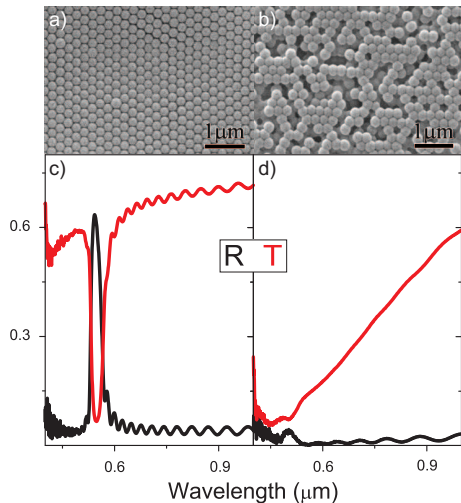


FIG. 1: Top panel: SEM images of photonic crystal with 0% (a) and 40% (b) vacancy doping. (c) and (d) reflection and transmission from the corresponding samples of the above panel.

The scattering mean free path in a random medium can be shown to be  $\ell_s = 1/\rho_s\sigma$ , where  $\sigma$  is the scattering cross-section and  $\rho_s$  is the scatterers number density [9].  $\ell_s$  is not only a measure of the quality of a photonic structure but also the basic length-scale of a more complex picture of multiple scattering and light diffusion. While quantities like the transport mean free path or the diffusion constant are meaningful only in the context of the diffusion approximation,  $\ell_s$  has a full meaning in any microscopic picture, regardless of the transport regime.

In our system, the degree of extrinsic disorder (see scanning electron microscopy (SEM) images in Fig. 1a and 1b) can be very precisely and uniformly tuned, while keeping the sample thickness controlled. This allows us to develop a setup to measure Lambert-Beer's law for photonic crystals. We used a Fourier transform spectrometer coupled to a microscope allowing to probe the scattering in the (111) direction while illuminating a constant-thickness area with a spot of  $\sim 80 \mu\text{m}$ . The spectra (see figures 1c and 1d) are taken in adjacent regions which are visible by optical microscope inspection as terraces on the sample surface. The thickness of such layers is precisely measured with an uncertainty of 2%, via the density of Fabry-Perot fringes that occur for the interference of the light reflected from the front and rear faces of the sample.

Figure 2a shows the measured  $\ln(T+R)$  for three different degrees of vacancy doping [7] i.e. for different degrees of extrinsic disorder, at a wavelength of 633 nm and for spheres of 237 nm in diameter ( $a/\lambda = 0.52$ ). In this type of representation, the slope yields directly  $(-\ell_s)^{-1}$  according to Eq. 1. This wavelength is chosen to exem-

plify a spectral region where no photonic band features are present, as, at such a low energy, the photonic crystal band dispersion is the same as in a uniform homogeneous effective medium. In figure 2a three scattering regimes are clearly distinguishable. For thicknesses lower than *ca.* 10 layers, (regime I), up to  $\sim 25 - 30\%$  of the incident light is scattered due to surface effects, in the form of stacking patterns [22], high lattice displacements and, even stacking order arrangements [23]. When the second regime (II) sets in, the slope  $\ell_s^{-1}$  reaches a stationary value that characterises the photonic crystal. Eq. 1 holds and scattering losses scale with sample thickness like  $\sim \exp(L/\ell_s)$ . Finally, for larger thicknesses, a third scattering regime (III) appears in Fig. 2a. Apparently, for thick samples  $> 50$  layers, the self-assembling process loses its effectiveness, as it evident by the increase of intrinsic disorder and by the cracks that appear on thick sample as they start to lift from the substrate.

The physical picture we propose can be checked against consistency if additional disorder is added to the photonic crystals. This can be done by doping the original photonic crystal with a controlled concentration of vacancies. At a wavelength of 633 nm the values of  $\ell_s$ , calculated from the fit to the Lambert-Beer law, are plotted as a function of vacancy density in Fig. 2b. The "perfect" crystal (that with 0% added vacancies) is highly ordered as it presents a scattering mean free path of 63  $\mu\text{m}$ , hundreds of times the lattice constant (in this case  $a = 0.33 \mu\text{m}$ ), and in particular much larger than the Bragg length (of the thick sample) [24] that in our case is  $L_B = (3.8 \pm 0.3) \mu\text{m}$ . An addition of a very little amount of defects rapidly decreases the mean free path,

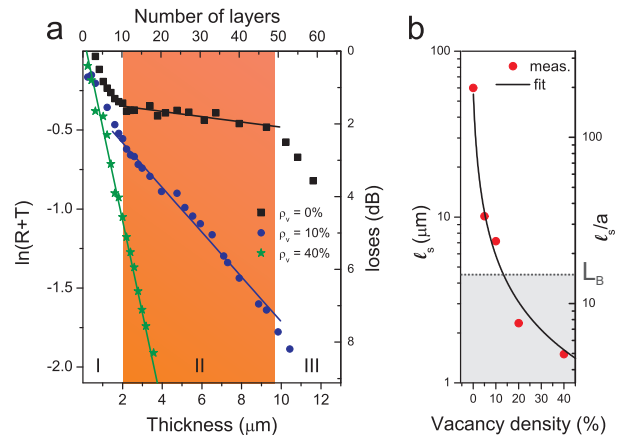


FIG. 2: (a) Plot of  $\ln(R+T)$  as a function of the sample thickness, at  $\lambda = 633 \text{ nm}$ , for different vacancy density doped photonic crystals (from 0% to 40% vacancies doping), of 237 nm diameter. (b)  $\ell_s$  obtained from linear fitting of the slope, for regime II. It also shows the Bragg length ( $L_B$ ) in the case of  $\rho_v = 0\%$  as shaded area.

hence the quality of the crystal. In this figure, the inverse scattering mean free path scales linearly with the vacancy concentration  $\rho_v$ , as shown by the black line, which is a fit for  $\ell_s^{-1} = \rho_0\sigma_0 + \rho_v\sigma_v$  where  $\rho_0$  and  $\rho_v$  are the density of intrinsic and intentionally added scatterers and  $\sigma_0$  and  $\sigma_v$  their scattering cross-section respectively. From the fit of  $\ell_s(\rho_v)$  as a function of the vacancy concentration we can estimate  $\sigma_v = (0.016 \pm 0.002) \mu\text{m}^2$ .

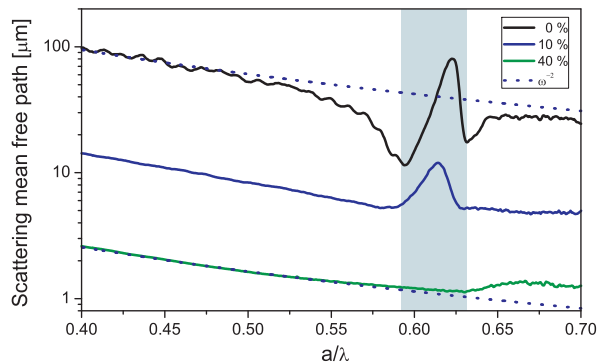


FIG. 3: Figure shows  $\ell_s$  as a function of the light wavelength for 0%, 10% and 40% vacancy doped photonic crystals with  $d = 237$  nm. The position of the pseudo-gap is shaded in cyan. The dotted line shows the  $\omega^{-2}$  dependence of  $\ell_s$  far from the band-gap.

Fig. 3 shows the strong chromatic dispersion of  $\ell_s(\omega)$  in the visible range. This is the signature of the photonic crystal. In the low energy side of the pseudo-bandgap,  $\ell_s$  takes on a value of the order of  $\sim 100 \mu\text{m}$  for sphere diameter  $d = 237$  nm and  $\sim 500 \mu\text{m}$  for  $d = 600$  nm (not shown here), the largest values reported so far. Previous experiments [15, 16, 17] have measured  $\ell_t$ , the transport mean free path, from very thick ( $\sim 200 \mu\text{m}$ ) photonic crystals grown by natural sedimentation [16, 17] or centrifugation [15], and found values in the range  $7 \mu\text{m} < \ell_t < 20 \mu\text{m}$ .  $\ell_s$  is in general smaller than  $\ell_t$  and, therefore, the values found in our experiment represent a much higher degree of ordering than previous reports. Far from the band-gap,  $\ell_s(\omega)$  varies as  $\sim \omega^{-2}$ , dependence that has been confirmed also in previous experiments [15] and attributed to Rayleigh-Gans type of scattering.

A simple model for a point-like scatterer in a photonic crystal can explain the chromatic dispersion of  $\ell_s$ . We assume that the scattering is isotropic and, therefore, that the imaginary part of the green tensor  $\mathbb{G}(\mathbf{r}, \mathbf{r}')$  can be approximated by  $\text{Im}\{\mathbb{G}(\mathbf{r}, \mathbf{r}')\} \sim (\pi c^2/2\omega)\mathcal{D}(\mathbf{r}, \omega)\mathbb{I}$ . We denote the  $\mathbf{k}$  contribution to the local density of states (or "projected" density of states) by  $\mathcal{D}_{\mathbf{k}}(\mathbf{r}, \omega)$ , and calculating the power radiated by a dipole we obtain a (spatially averaged) scattering cross section

$$\sigma_{\mathbf{k}}(\omega) \sim F(\omega)\omega^2\mathcal{D}(\omega)\mathcal{D}_{\mathbf{k}}(\omega), \quad (2)$$

where  $F(\omega)$  is a form factor which takes into account corrections beyond Rayleigh scattering and  $\mathbf{k}$  the wavevec-

tor in the incident direction. In our simple model, the form factor can be replaced by a Rayleigh-Gans factor  $F(\omega) \sim \omega^{-2}$  and the polarizability of the scatterer can be considered independent of frequency [15]. Eq. 2 states that the scattering cross-section, and hence the scattering mean free path, has a strong dependence on the total  $\mathcal{D}(\omega)$  and projected  $\mathcal{D}_{\mathbf{k}}(\omega)$ . This dependence typically disappears in ordinary random media for which the photonic modes are isotropic and energetically smooth, but is very important for photonic crystals. At the band-edges of our photonic crystals,  $\ell_s(\omega)$  has a sharp decrease of a factor of up 4 to  $\ell_s(a/\lambda = 0.59) = 11 \pm 1 \mu\text{m}$  and then it shoots up almost an order of magnitude in the band-gap to  $\ell_s(a/\lambda = 0.62) = 81 \pm 40 \mu\text{m}$ . Such an 8-fold increase occurs within just 0.03 in  $a/\lambda$  and  $\sim 27$  nm in wavelength, around the photonic band-gap. Again, as a comparison, we show in Fig. 3 the frequency dependence of  $\ell_s$  for the 10% and the 40% vacancy photonic crystal, the latter can be considered fully disordered. As the vacancy doping is increased, the profile is smoothed. Firstly the band-edge effect on  $\ell_s$  disappears, as these standing-wave-like states are very sensitive to disorder. Then, for the 40% vacancy case, the effects on  $\mathcal{D}(\omega)$  are washed out and the only feature in  $\ell_s$  occurs at the position of the first Mie resonance of the individual dielectric spheres [19]. This weak energy dependence of  $\ell_s$  is likely to be the only residual effect in a very disordered opal, as those grown by natural sedimentation or centrifugation [15, 16, 17], which present superficial iridescence but are largely bulk-disordered and exhibit standard light diffusion.

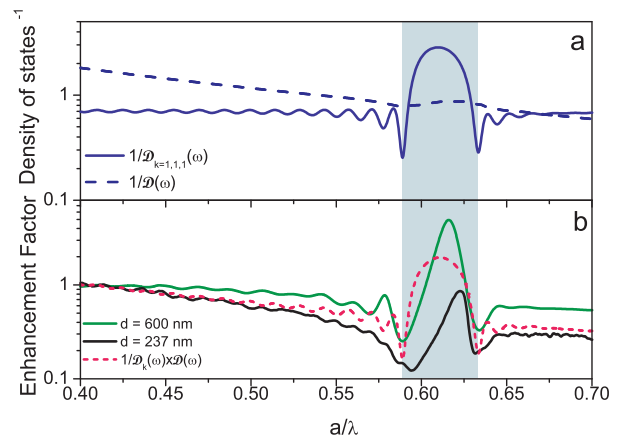


FIG. 4: (a) Inverse of the total  $\mathcal{D}(\omega)$  and the projected  $\mathcal{D}_{k=(1,1,1)}(\omega)$  along the incident direction ( $\Gamma - L$  direction) are plotted. (b) Enhancement factor,  $\ell_s(a/\lambda) / \ell_s(a/\lambda = 0.4)$ , for two opals with no vacancy doping and the product  $(\mathcal{D}_{\mathbf{k}}(\omega) - 1)$ . The position of the pseudo-gap is shaded in cyan.

Figure 4a shows the inverse of the total density of states (dark blue dotted line) that has a very weak mod-

ulation at the gap together with  $\mathcal{D}_{\mathbf{k}}(\omega)$  for propagation parallel to  $\mathbf{k} = (111)$  that does have a strong variation at the gap (violet full line).  $\mathcal{D}_{\mathbf{k}}(\omega)$  is calculated from the inverse of the group velocity [25]  $v_G(111)$  from ref. [26].

Figure 4b shows the enhancement factor defined as the ratio of  $\ell_s$  to its value far from the gap,  $\ell_s(a/\lambda)/\ell_s(a/\lambda = 0.4)$ , for two different samples composed by PMMA spheres of 237 nm (black curve) and 600 nm (green curve) in diameter respectively. The enhancement factor points out the existence of a photonic pseudo-gap and reveals the variation of the density of states in the photonic crystal. A clear resonant behavior is evident. The variation in  $\ell_s$  is 8-fold for  $d = 237$  nm and 20-fold for  $d = 600$  nm, which we attribute to the superior quality of the lattice. In figure 4b we plot also  $1/\mathcal{D}(\omega)\mathcal{D}(\omega)_{\mathbf{k}}$  (dashed pink curve) that, from Eq. 2, is expected to reproduce the shape of energy dependence of  $\ell_s(\omega)$ . A fair agreement between theory and experiment is obtained, and the qualitative behavior is well captured by our simple model. Although both  $\mathcal{D}(\omega)$  and  $\mathcal{D}_{\mathbf{k}}(\omega)$  contribute to the strong variation of  $\ell_s$ , it is evident that the principal factor responsible for a change in  $\ell_s$  (111) is  $\mathcal{D}_{\mathbf{k}}(\omega)$ .

Our simple and qualitative model accounts remarkably well for the shape of the measured  $\ell_s(\omega)$  although it does not account for the asymmetry of its dispersion in the photonic gap. This effect is related to the available scattering states in other crystallographic directions close to the incident one [27]. Our measurement indicates the need for a more complete theoretical model that should account for all the modes in all directions with the right scattering probability.

An increase of  $\ell_s$  in the band-gap and a decrease at the band-edge reflects the modified phase space available  $\Delta k$  for light scattering when the photonic modes are concentrated around few  $k$ -directions or the available scattered states reduced. This is consistent with John's seminal prediction of a need for a modified Ioffe-Regel criterion [2] for scattering in photonic crystals, to include  $\Delta k$ . In addition, here we show that as the phase-space is modified, also  $\ell_s$  is altered: light scattering in photonic crystals is richer than in conventional amorphous media. Complete photonic band-gap materials, like Si inverted opals, would amplify the effect here presented and could be proper candidates to observe Anderson localisation of light.

In conclusion, we show that a controlled smooth transition from ballistic to diffuse transport in photonic crystals can be induced by the introduction of extrinsic disorder. We find that the strength of scattering is closely related to the density of states, which induces immense, up to 20-fold, variations in the scattering mean free path. We propose  $\ell_s$  as a robust, easy to measure, figure of merit in assessing the quality of photonic crystals for technological applications. The possibility of controlling light scattering and diffusion in nano-structured optical

media has important implications not only to test the quality of photonic devices, but also to properly address the proximity to the onset of Anderson localization in disordered lattices, or for the spectral control of lasing emission from disordered/ordered active media [10].

We thank J.F. Galisteo-López for the data of the group velocity and J. J. Sáenz for fruitful discussion. We are also indebted to D. Delande, M. Artoni and Ad Lagendijk for invaluable advice. LSFP acknowledges the financial support of the Spanish Ministry of Science and Innovation through its Juan de la Cierva program. The work was supported by the EU through Network of Excellence IST-2-511616-NOE (PHOREMOST), CI-CyT NAN2004-08843-C05, MAT2006-09062, the Spanish MEC Consolider-QOIT CSD2006-0019 and the Comunidad de Madrid S-0505/ESP-0200.

- 
- [1] E. Yablonovitch, Phys. Rev. Lett. 58, 2059 (1987)
  - [2] S. John, Phys. Rev. Lett. 58, 2486 - 2489 (1987)
  - [3] P. Lodahl *et al.*, Nature 430, 654 - 657 (2004); S. Noda *et al.* Nature Photonics 1, 449 - 458 (2007); A. F. Koenderink and W.L. Vos, Phys. Rev. Lett. 91, 213902 (2003)
  - [4] C. Toninelli *et al.* Phys. Rev. Lett. 101, 123901 (2008)
  - [5] L. F. Rojas-Ochoa *et al.* Phys. Rev. Lett. 93, 073903 (2004)
  - [6] P. Sheng, *Introduction to Wave Scattering, Localization, and Mesoscopic Phenomena* (Academic Press, San Diego, 1995)
  - [7] P. D. García *et al.* Adv. Mater. 19,2597-2602 (2007).
  - [8] P. Barthelemy *et al.* Nature **453**, 495 (2008)
  - [9] E. Akkermans and G. Montambaux, *Mesoscopic Physics of Electrons and Photons* (Cambridge University Press, Cambridge, 2007)
  - [10] D.S. Wiersma, Nature Physics **4** 359 (2008); S. Gottardo *et al.*, Nature Photonics, 2, 429, (2008).
  - [11] R. Carminati *et al.*, arXiv:0810.1411 (October 2008)
  - [12] P.W Anderson, Phys. Rev., 109, 1492 - 1505 (1958).
  - [13] D. Wiersma *et al.* Nature, 390, 671, (1997); M. Stoezner *et al.* Phys. Rev. Lett., 96, 063904 (2006); A. A. Chabanov *et al.* Nature 404, 850-853 (2000).
  - [14] T. Schwartz *et al.* Nature 446, 52 (2007)
  - [15] A. F. Koenderink *et al.* Physics Letters A 268, 104 (2000); J. Huang *et al.* Phys. Rev. Lett. 86, 4815 - 4818 (2001)
  - [16] V. N. Astratov, Nuovo Cimento D 17D, 1349 1995.
  - [17] Y. A. Vlasov *et al.* Phys. Rev. B 60, 1555 - 1562 (1999)
  - [18] A. F. Koenderink *et al.* Phys. Rev. B 72, 153102 (2005)
  - [19] R. Sapienza *et al.*, Phys. Rev. Lett. 99, 233902 (2007)
  - [20] F. García-Santamaría *et al.* Phys. Rev. B 71 (19), 195112 (2005)
  - [21] P. Jiang *et al.* Chem. Mater. 1999, 11, 2131.
  - [22] X. Checoury *et al.* Appl. Phys. Lett. 90,161131 (2007).
  - [23] N.D. Denkov *et al.*, Langmuir 8, 3183 (1992).
  - [24] J.F. Galisteo-López *et al.*, Phys. Rev. B 68, 115109 (2003).
  - [25] B. Balian and C. Bloch, Ann. Phys., 64, 271, 1971.
  - [26] J.F. Galisteo-López *et al.*, Phys. Rev. B 73, 125103 (2006)
  - [27] M.A. Kaliteevskii *et al.*, Phys. Rev. B, 66, 113101 (2002).